REFERENCES

Bhattacharyya, D., Bej, S.K. and Rao, M.S., "Oxidative dehydrogenation of n-butane to butadiene. Effect of different promoters on the performance of vanadium-magnesium oxide catalysts", *Appl. Catal.*, **87** (1992) 29.

Blasco,T. and Nieto, J.M.L., "Oxidative dehydrogenation of short chain alkanes on supported vanadium oxide catalyst", *Appl. Catal.*, **157** (1997) 117.

Bond, G.C. and Tahir, S.F., "Vanadium oxide monolayer catalysts. Preparation, characterization and catalytic activity", *Appl. Catal.*, **71** (1991)1.

Busca, G., "Infrared studies of the reactive adsorption of organic molecules over metal oxides and of the mechanisms of their heterogeneously-catalyzed oxidation", *Catal. Today*, **27** (1996) 457.

Cavani, F. and Trifiro, F., "The oxidative dehydrogenation of ethane and propane as an alternative way for the production of light olefins", *Catal. Today*, **24** (1995) 307.

Chaar, M.A., Patel, D., Kung, M.C. and Kung, H.H., "Selective oxidative dehydrogenation of butane over V-Mg-O catalysts", *J. Catal.*, **105** (1987) 483.

Chaar, M.A., Patel D. and Kung, H.H., "Selective oxidative dehydrogenation of propane over V-Mg-O catalyst", *J.Catal.*, **109** (1988) 463.

Corma, A., Nieto, J.M.L. and Paredes, N., "Preparation of V-Mg-O catalysts: Nature of active species precursors", *Appl. Catal.*, **104** (1993a) 161.

Corma, A., Nieto, J.M.L. and Paredes, N., "Influence of the preparation methods of V-Mg-O catalysts on their catalytic properties for the oxidative dehydrogenation of propane", *J. Catal.*, **144** (1993b) 425.

Courcot, D., Ponchel, A., Grzybowska, B., Barbaux, Y., Rigole, M and Guelton, M., "Effect of potassium addition to the TiO_2 support on the structure of V_2O_5/TiO_2 and its catalytic properties in the oxidative dehydrogenation of propane", *J. Chem. Soc., Faraday Trans.*, **92**(9) (1996) 1609.

Courcot, D., Ponchel, A., Grzybowska, B., Barbaux, Y., Rigole, M., Guelton, M. and Bonnelle, J.P., "Effect of the sequence of potassium introduction to V_2O_5/TiO_2 catalysts on their physicochemical properties and catalytic

performance in oxidative dehydrogenation of propane", *Catal. Today*, **33** (1997) 109.

Galli, A. and Nieto, J.M.L., "The effect of potassium on the selective oxidation of n-butane and ethane over Al_2O_3-supported vanadia catalysts", *Catal. Lett.*, **34** (1995) 51.

Gao, X., Ruiz, P., Xin, Q., Guo, X., and Delmon, B., "Preparation and characterization of three pure magnesium vanadate phases as catalysts for selective oxidation of propane to propene", *Catal. Lett.*, **23** (1994) 321.

Grzybowska-Swierkosz, B., " Vanadia-titania catalysts for oxidation of *o*-xylene and other hydrocarbons", *Appl. Catal.*, **157** (1997) 263.

Guerrero-Ruiz, A., Ramos, I.R., Freno, J.L.G., Soenen, V., Herrmann, J.M. and Volta, J.C., Stud. in Surf. Sci. and Catal., Elsevier, Amsterdam, **72** (1992) 203.

Guerrero-Ruiz, A., Rodriguez-Ramos, I., Ferreira-Aparicia, P. and Volta, J.C., "Study of surface and lattice oxygen atoms over magnesium vanadate phases by isotopic exchange with $C^{18}O_2$", *Catal Lett.*, **45** (1997) 113.

Kanokrattana, O., "Effect of alkali metals on V-Mg-O catalyst in the oxidative dehydrogenation of propane", *Master of Engineering thesis*, Chulalongkorn University, (1997).

Khodakov, A., Olthof, B., Bell, A.T. and Iglesia, E., "Structure and catalytic properties of supported vanadium oxides: Support effects on oxidative dehydrogenation reactions", *J. Catal.*, **181** (1999) 205.

Kung, M.C. and Kung, H.H., "The effect of potassium in the preparation of magnesium orthovanadate and pyrovanadate on the oxidative dehydrogenation of propane to propene", *J. Catal.*, **134** (1992) 668.

Kung, M.C. and Kung, H.H., "Oxidative dehydrogenation of alkanes over vanadium-magnesium-oxides", *Appl. Catal.*, **157** (1997) 105.

Machej, T., Haber, J., Turek, A.M. and Wachs, T.E., "Monolayer V_2O_5/TiO_2 and MoO_3/TiO_2 catalysts preparation by different methods", *Appl. Catal.*, **70** (1991) 115.

Morrison, R.T. and Boyd, R.N., *Organic Chemistry*, 6th ed., Simon and Schuster Company, Englewood Cliffs, New Jersey, (1992).

Nguyen, K.T. and Kung, H.H., "Analysis of the surface-enhanced homogeneous reaction during oxidative dehydrogenation of propane over a V-Mg-O catalyst", *Ind. Eng. Chem. Res.*, **30** (1991) 352.

Nieto, J.M.L., Kremenic, G. and Fierro, J.L.G., "Selective oxidation of propene over supported vanadium oxide catalysts. *Appl. Catal.*, 61 (1990) 235.

Owen, O.S., Kung, M.C. and Kung, H.H., "The effect of oxide structure and cation reduction potential of vanadates on the selective oxidative dehydrogenation of butane and propane", *Catal. Lett.*, **12** (1992) 45.

Perry, R.H. and Chilton, C.H., *Chemical Engineers' Handbook*, McGraw-Hill International Book Company, 5th ed., 1973

Ramis, G., Busca, G. and Bregani, F., "On the effect of dopants and additives on the state of surface vanadyl centers of vanadia-titania catalysts", *Catal. Lett.*, **18** (1993) 299.

Reid, Robert, C., Prausnitz, John, M., and Poling Bruce, E., *The Properties of Gases and Liquids*, McGraw-Hill International Book Company, 4th ed., 1988

Sam, D.S.H., Soenen, V. and Volta, J.C., "Oxidative dehydrogenation of propane over V-Mg-O catalysts", *J. Catal.*, **123** (1990) 417.

Teratrakoonwichaya, S., "The development of nitric oxide removal catalysts for exhaust gases from stationary source", *Master of Engineering thesis*, Chulalongkorn University, (1996).

Thammanonkul, H., "Oxidative dehydrogenation of propane over V-Mg-O catalysts", *Master of Engineering thesis*, Chulalongkorn University, (1996).

Wachs, I.E., Jehng, J.M., Deo, G., Weckhuysen, B.M., Guliants, V.V., Benziger, J.B., "In situ Raman spectroscopy studies of bulk and surface metal oxide phases during oxidation reaction", *Catal. Today*, **32** (1996a) 47.

Wachs, I.E., Deo, G., Weckhuysen, B.M., Andreini, A., Vuurman, M.A., De Boer, M. and Amiridis M.D., "Selective catalytic reduction of NO with NH_3 over supported vanadia catalysts", *J. Catal.*, **161** (1996b) 211.

Wachs, I.E., Weckhuysen, B.M., " Structure and reactivity of surface vanadium oxide species on oxide supports", *Appl. Catal.*, **157** (1997) 67.

Zazhigalov, V.A., Haber, J., Stoch, J., Bacherikova, I.V., Komashko, G.A. and

Pyatnitskaya, A.I., "n-Butane oxidation on V-P-O catalysts. Influence of alkali and alkali earth metal ions as additions", *Appl. Catal.*, **134** (1996) 225.

APPENDIX A

CALCULATION OF CATALYST PREPARATION

A.1 Calculation for the preparation of the 5VTi catalyst

The aqueous solution used for catalyst preparation consists of 0.4 wt% NH_4VO_3. The volume of this solution is designed to be 50 ml., hence NH_4VO_3 and H_2O are weighted for 0.2 and 49.8 gram, respectively.

$$\text{the amount of V in 0.2 g of } NH_4VO_3 = \frac{0.2 \times 50.9414}{116.98}$$

$$\approx 0.0871 \text{ g}$$

$$\text{therefore, mole of V} = \frac{0.0871}{50.9414}$$

$$\approx 0.0017 \text{ mole}$$

$$\text{the amount of V calculated as } V_2O_5 = \frac{0.0871 \times 181.8828}{101.8828}$$

$$\approx 0.1555 \text{ g}$$

If the weight of catalyst is 100 gram. 5VTi would compose of 5 g of V_2O_5 and 95 g of TiO_2. Thus, in this system,

$$\text{the amount of } TiO_2 = \frac{95 \times 0.1555}{5}$$

$$\approx 2.9545 \text{ g}$$

A.2 Calculation for the preparation of co-5V1MgTi, 1Mg5VTi and 5V1MgTi catalysts

The calculation for vanadia loading is similar to the above calculation, except the calculation of Mg loading. The Mg content is calculated in terms of V/Mg atomic

ratio which is fixed to be 1/1. Therefore, from the above calculation, the mole of Mg would be equal to 0.0017 mole.

$$\text{the amount of Mg} = 0.0017\times24.305$$
$$\approx 0.0416\ \text{g}$$

Mg is impregnated from $Mg(NO_3)_2$ solution

$$\text{thus, the amount of } Mg(NO_3)_2 \text{ used} = \frac{0.0416\times256.41}{24.305}$$
$$\approx 0.4384\ \text{g}$$

If the weight of V_2O_5 plus TiO_2 is assumed to be 100 gram, thus,

$$\text{there is magnesium in 5 wt\% } V_2O_5/TiO_2 = \frac{0.0416}{(0.1555+2.9545)}\times100\%$$
$$\approx 1.3\ \%$$

A.3 Calculation for the preparation of 5V2MgTi catalyst

The calculation for 5V2MgTi preparation is the same as 5V1MgTi but the V/Mg atomic ratio is changed from 1/1 to 2/3.

$$\text{therefore, the mole of Mg} = \frac{2}{3}\times0.0017$$
$$\approx 0.00256\ \text{mole}$$
$$\text{the amount of Mg used} = 0.00256\times24.305$$
$$\approx 0.0623\ \text{g}$$
$$\text{thus the amount of } Mg(NO_3)_2 = \frac{0.0623\times256.41}{24.305}$$
$$\approx 0.6576\ \text{g}$$
$$\text{there is magnesium in 5V2MgTi} = \frac{0.0623}{(0.1555+2.9545)}\times100\%$$
$$\approx 2.0\%$$

A.4 Calculation for the preparation of 3V2MgTi catalyst

The vanadia aqueous solution consists of 0.2 wt% of NH_4VO_3. The volume of this solution is 50 ml. Thus it composes of 0.1 g of NH_4VO_3 and 49.9 g of H_2O.

$$\text{the amount of V in the catalyst} = \frac{0.1 \times 50.9414}{116.98} \approx 0.0435 \text{ g}$$

$$\text{the mole of V} = \frac{0.0435}{50.9414} \approx 0.00085 \text{ mole}$$

$$\text{the amount of V calculated as } V_2O_5 = \frac{0.0435 \times 181.8828}{101.8828} \approx 0.0777 \text{ g}$$

If the catalyst is assumed that it composes of only V_2O_5 and TiO_2. In 100 gram of catalyst, it would compose of 3 g of V_2O_5 and 97 g of TiO_2 (3 wt%V_2O_5/TiO_2). Thus, in this system;

$$\text{the amount of } TiO_2 = \frac{97}{3} \times 0.0777 \approx 2.5123 \text{ g}$$

Then 2 wt % of Mg is added onto the catalyst (when the weight of V_2O_5 plus TiO_2 is calculated as 100%).

$$\text{the amount of Mg in 5V2MgTi} = 0.02 \times (0.0777 + 2.5123) \approx 0.0519 \text{ g}$$

$$\text{the amount of } Mg(NO_3)_2 \text{ used} = \frac{0.0519 \times 256.41}{24.305} \approx 0.5473 \text{ g}$$

A.5 Calculation for the preparation of 10V2MgTi catalyst

The step of calculation of 10V2MgTi is the same of 3V2MgTi, except the amount of V_2O_5 is changed to 10 wt%. However, the amount of Mg is still 2 wt%. The volume of vanadia aqueous solution is 50 ml which have 0.2 g of NH_4VO_3 and 49.8 g of H_2O. Thus, from the calculation for the preparation of 5VTi catalyst, the amount of V_2O_5 is 0.1555 g

thus, the amount of TiO_2 $= \frac{90}{10} \times 0.1555$

$\approx$ 1.3995 g

the amount of Mg $= 0.02 \times (0.1555+1.3995)$

$\approx$ 0.0311 g

the amount of $Mg(NO_3)_2$ used $= \frac{0.0311 \times 256.41}{24.305}$

$\approx$ 0.3286 g

APPENDIX B

CALCULATION OF DIFFUSIONAL LIMITATION EFFECT

In the present work there is doubt whether the external and internal diffusion limitations interfere with the 1-propanol oxidation reaction. Hence, the kinetic parameters were calculated based on the experimental data so as to prove the controlled system. The calculation is divided into two parts; one of which is the external diffusion limitation, and the other is the internal diffusion limitation.

B1. External diffusional limitation

The 1-propanol oxidation reaction is considered to be an irreversible first order reaction occurred on the interior pore surface of catalyst particles in a fixed bed reactor. Assume isothermal operation for the reaction.

In the experiment, 4% 1-propanol in air was used as the unique reactant in the system. Molecular weight of 1-propanol and air are 60 and 29, respectively. Thus, the average molecular weight of the gas mixture was calculated as follows:

$$M_{AB} = 0.04\times60 + 0.96\times0.29$$
$$= 30.24 \text{ g/mol}$$

Calculation of reactant gas density

Consider the 1-propanol oxidation is operated at low pressure and high temperature. We assume that the gases are respect to ideal gas law. The density of such gas mixture reactant at various temperatures is calculated in the following.

We obtained : $\rho = 0.779$ kg/m^3 at T = 200°C

$\rho = 0.705$ kg/m^3 at T = 250°C

$\rho = 0.643$ kg/m^3 at T = 300°C

$\rho = 0.592$ kg/m^3 at T = 350°C

Calculation of the gas mixture viscosity

The simplified methods for determining the viscosity of low pressure binary are described anywhere [Reid (1988)]. The method of Wilke is chosen to estimate the gas mixture viscosity.

For a binary system of species 1 and species 2,

$$\mu_m = \frac{y_1\mu_1}{y_1 + y_2\phi_{12}} + \frac{y_2\mu_2}{y_2 + y_1\phi_{21}}$$

where μ_m = viscosity of the mixture

μ_1, μ_2 = pure component viscosity

y_1, y_2 = mole fractions

$$\phi_{12} = \frac{\left[1+\left(\frac{\mu_1}{\mu_2}\right)^{1/2}\left(\frac{M_2}{M_1}\right)^{1/4}\right]}{\left[8\left(1+\frac{M_1}{M_2}\right)\right]^{1/2}}$$

$$\phi_{21} = \phi_{12}\left(\frac{\mu_2}{\mu_1}\right)\left(\frac{M_1}{M_2}\right)$$

M_1, M_2 = molecular weight

Let 1 refer to 1-propanol and 2 to air

$M_1 = 60$ and $M_2 = 29$

From Perry [Perry (1973)] the viscosity of pure 1-propanol at 200°C , 250°C , 300°C and 350°C are 0.0124, 0.0135, 0.015 and 0.0162 cP, respectively. The viscosity of pure air at 200°C, 250°C, 300°C and 350°C are 0.0248, 0.0265, 0.0285 and 0.030 cP, respectively.

At 200°C :

$$\phi_{12} = \frac{\left[1+\left(\frac{0.0124}{0.0248}\right)^{1/2}\left(\frac{29}{60}\right)^{1/4}\right]^2}{\left[8\left(1+\frac{60}{29}\right)\right]^{1/2}} = 0.510$$

$$\phi_{21} = 0.510\left(\frac{0.0248}{0.0124}\right)\left(\frac{60}{29}\right) = 2.110$$

$$\mu_m = \frac{0.04\times 0.0124}{0.04+0.96\times 0.510} + \frac{0.96\times 0.0248}{0.96+0.04\times 2.110} = 0.0237\,\text{cP} = 2.37\times 10^{-5}\,\text{kg/m}-\text{sec}$$

At 250°C :

$$\phi_{12} = \frac{\left[1+\left(\frac{0.0135}{0.0265}\right)^{1/2}\left(\frac{29}{60}\right)^{1/4}\right]^2}{\left[8\left(1+\frac{60}{29}\right)\right]^{1/2}} = 0.514$$

$$\phi_{21} = 0.514\left(\frac{0.0265}{0.0135}\right)\left(\frac{60}{29}\right) = 2.086$$

$$\mu_m = \frac{0.04\times 0.0135}{0.04+0.96\times 0.514} + \frac{0.96\times 0.0265}{0.96+0.04\times 2.086} = 0.0254\,\text{cP} = 2.54\times 10^{-5}\,\text{kg/m}-\text{sec}$$

At 300°C :

$$\phi_{12} = \frac{\left[1+\left(\frac{0.015}{0.0265}\right)^{1/2}\left(\frac{29}{60}\right)^{1/4}\right]^2}{\left[8\left(1+\frac{60}{29}\right)\right]^{1/2}} = 0.52$$

$$\phi_{21} = 0.52\left(\frac{0.0265}{0.015}\right)\left(\frac{60}{29}\right) = 2.043$$

$$\mu_m = \frac{0.04\times 0.015}{0.04+0.96\times 0.52} + \frac{0.96\times 0.0265}{0.96+0.04\times 2.043} = 0.0274\,\text{cP} = 2.74\times 10^{-5}\,\text{kg/m}-\text{sec}$$

At 350^0C :

$$\phi_{12} = \frac{\left[1+\left(\frac{0.0162}{0.030}\right)^{1/2}\left(\frac{29}{60}\right)^{1/4}\right]^2}{\left[8\left(1+\frac{60}{29}\right)\right]^{1/2}} = 0.525$$

$$\phi_{21} = 0.525\left(\frac{0.030}{0.0162}\right)\left(\frac{60}{29}\right) = 2.011$$

$$\mu_m = \frac{0.04\times 0.0162}{0.04+0.96\times 0.525} + \frac{0.96\times 0.030}{0.96+0.04\times 2.011} = 0.0289\,\text{cP} = 2.89\times 10^{-5}\,\text{kg/m}-\text{sec}$$

Calculation of diffusion coefficients

Diffusion coefficients for binary gas system at low pressure calculated by empirical correlation are proposed by Reid (1988). Wilke and Lee method is chosen to estimate the value of D_{AB} due to the general and reliable method. The empirical correlation is

$$D_{AB} = \frac{\left(3.03-\frac{0.98}{M_{AB}^{1/2}}\right)(10^{-3})T^{3/2}}{PM_{AB}^{1/2}\sigma_{AB}^2\Omega_D}$$

where D_{AB} = binary diffusion coefficient,cm^2/s

T = temperature, K

M_A ,M_B = molecular weights of A and B, g/mol

$$M_{AB} = 2\left[\left(\frac{1}{M_A}\right)+\left(\frac{1}{M_B}\right)\right]^{-1}$$

P = pressure,bar

σ = characteristic length,^{o}A

Ω_D = diffusion collision integral , dimensionless

The characteristic Lennard-Jones energy and Length, ε and σ, of 1-propanol and air are as follows: [Reid (1988)]

For 1-propanol: $\sigma(C_3H_7OH) = 4.549\ ^{\circ}A$, $\varepsilon/k = 576.7$

For air : $\sigma(air) = 3.711\ ^{\circ}A$, $\varepsilon/k = 78.6$

The simple rules are usually employed.

$$\sigma_{AB} = \frac{\sigma_A + \sigma_B}{2} = \frac{4.549 + 3.711}{2} = 4.13$$

$$\varepsilon_{AB}/k = \left(\frac{\varepsilon_A \varepsilon_B}{k^2}\right)^{1/2} = (576.7 \times 78.6)^{1/2} = 212.9$$

Ω_D is tabulated as a function of $k/T\varepsilon$ for the Lennard-Jones potential. The accurate relation is

$$\Omega_D = \frac{A}{(T^*)^B} + \frac{C}{\exp(DT^*)} + \frac{E}{\exp(FT^*)} + \frac{G}{\exp(HT^*)}$$

where $T^* = \frac{kT}{\varepsilon_{AB}}$, A = 1.06036, B = 0.15610, C = 0.19300, D = 0.47635,

E = 1.03587 , F = 1.52996 , G = 1.76474 , H = 3.89411

Then $T^* = \frac{473}{212.9} = 2.222$ at 200°C

$T^* = \frac{523}{212.9} = 2.456$ at 250°C

$T^* = \frac{573}{212.9} = 2.691$ at 300°C

$T^* = \frac{623}{212.9} = 2.926$ at 350°C

$$\Omega_D = \frac{1.06036}{(T^*)^{0.15610}} + \frac{0.19300}{\exp(0.47635T^*)} + \frac{1.03587}{\exp(1.52996T^*)} + \frac{1.76474}{\exp(3.89411T^*)}$$

Ω_D = 1.038 ; 200°C

Ω_D = 1.006 ; 250°C

Ω_D = 0.979 ; 300°C

Ω_D = 0.956 ; 350°C

With Equation of D_{AB},

$$\text{At } 200^\circ\text{C} : D(C_3H_7OH\text{-air}) = \frac{\left(3.03 - \frac{0.98}{30.24^{0.5}}\right)(10^{-3})473^{3/2}}{1 \times 30.24^{0.5} \times 4.13^2 \times 1.038} = 3.01 \times 10^{-5} \quad m^2/s$$

$$\text{At } 250^\circ\text{C} : D(C_3H_7OH\text{-air}) = \frac{\left(3.03 - \frac{0.98}{30.24^{0.5}}\right)(10^{-3})523^{3/2}}{1 \times 30.24^{0.5} \times 4.13^2 \times 1.006} = 3.62 \times 10^{-5} \quad m^2/s$$

$$\text{At } 300^\circ\text{C} : D(C_3H_7OH\text{-air}) = \frac{\left(3.03 - \frac{0.98}{30.24^{0.5}}\right)(10^{-3})573^{3/2}}{1 \times 30.24^{0.5} \times 4.13^2 \times 0.979} = 4.26 \times 10^{-5} \quad m^2/s$$

$$\text{At } 350^\circ\text{C} : D(C_3H_7OH\text{-air}) = \frac{\left(3.03 - \frac{0.98}{30.24^{0.5}}\right)(10^{-3})623^{3/2}}{1 \times 30.24^{0.5} \times 4.13^2 \times 0.956} = 5.04 \times 10^{-5} \quad m^2/s$$

Reactant gas mixture was supplied at 100 ml/min. in tubular microreactor used in the 1-propanol oxidation system at 30°C

1-propanol flow rate through reactor = 100 ml/min. at 30°C

The density of 1-propanol , $\rho = \frac{1.0\times10^{5}\times30.24\times10^{-3}}{8.314(273+30)} = 1.216$ kg/m^3

Mass flow rate = $1.216\left(\frac{100\times10^{-6}}{60}\right) = 2.03\times10^{-6}$ kg/s

Diameter of quartz tube reactor = 6 mm

Cross-sectional area of tube reactor = $\frac{\pi(6\times10^{-3})^2}{4} = 2.83\times10^{-5}$ m^2

Mass Velocity , $G = \frac{2.03\times10^{-6}}{2.83\times10^{-5}} = 0.072$ kg/m^2-s

Catalysis size = 100-150 mesh = 0.178-0.126 mm

Average catalysis = (0.126+0.178)/2 = 0.152 mm

Find Reynolds number, Re_p , which is well known as follows :

$$Re_p = \frac{d_p G}{\mu}$$

We obtained

At 200°C : $Re_p = \frac{(0.152\times10^{-3}\times0.072)}{2.37\times10^{-5}} = 0.459$

At 250°C : $Re_p = \frac{(0.152\times10^{-3}\times0.072)}{2.54\times10^{-5}} = 0.429$

At 300°C : $Re_p = \frac{(0.152\times10^{-3}\times0.072)}{2.74\times10^{-5}} = 0.398$

At 350°C : $Re_p = \frac{(0.152\times10^{-3}\times0.072)}{3.0\times10^{-5}} = 0.377$

Average transport coefficient between the bulk stream and particles surface could be correlated in terms of dimensionless groups which characterize the flow conditions. For mass transfer the Sherwood number, $k_m\rho/G$, is an empirical function of the Reynolds number, d_pG/μ , and the Schmit number , $\mu/\rho D$. The j-factors are defined as the following functions of the Schmidt number and Sherwood numbers:

$$j_D = \frac{k_m \rho}{G}\left(\frac{a_m}{a_t}\right)(\mu / \rho D)^{2/3}$$

The ratio (a_m/a_t) allows for the possibility that the effective mass-transfer area a_m, may be less than the total external area, a_t, of the particles. For Reynolds number less than 10, the following relationship between j_D and the Reynolds number well represents available data.

$$j_D = \frac{0.458}{\varepsilon_B}\left(\frac{d_p G}{\mu}\right)^{-0.407}$$

where G = mass velocity(superficial) based upon cross-sectional area of empty reactor ($G = u\rho$)

d_p = diameter of catalyst particle for spheres

μ = viscosity of fluid

ρ = density of fluid

ε_B = void fraction of the interparticle space (void fraction of the bed)

D = molecular diffusivity of component being transferred

Assume $\varepsilon_B = 0.5$

At 200°C ; $j_D = \frac{0.458}{0.5}(0.459)^{-0.407} = 1.257$

At 250°C ; $j_D = \frac{0.458}{0.5}(0.429)^{-0.407} = 1.292$

At 300°C ; $j_D = \frac{0.458}{0.5}(0.398)^{-0.407} = 1.333$

At 350°C ; $j_D = \frac{0.458}{0.5}(0.377)^{-0.407} = 1.362$

A variation of the fixed bed reactor is an essembly of screens or gauze of catalytic solid over which the reacting fluid flows. Data on mass transfer from single screens has been reported by Gay and Maughan. Their correlation is of the form

$$j_D = \frac{\varepsilon k_m \rho}{G}(\mu / \rho D)^{2/3}$$

where ε is the porosity of the single screen.

Hence, $k_m = \frac{j_D G}{\rho}(\mu / \rho D)^{-2/3}$

$$k_m = \left(\frac{0.458G}{\varepsilon_B \rho}\right) Re^{-0.407} Sc^{-2/3}$$

Find k_m : At 200°C, $k_m = \left(\frac{1.257 \times 0.072}{0.779}\right)(0.541)^{-2/3} = 0.174$ m/s

At 250°C, $k_m = \left(\frac{1.292 \times 0.072}{0.705}\right)(0.601)^{-2/3} = 0.185$ m/s

At 300°C, $k_m = \left(\frac{1.333 \times 0.072}{0.643}\right)(0.663)^{-2/3} = 0.194$ m/s

At 350°C, $k_m = \left(\frac{1.362 \times 0.072}{0.592}\right)(0.723)^{-2/3} = 0.205$ m/s

Find Schmidt number, Sc: $Sc = \frac{\mu}{\rho D}$

At 200°C: $Sc = \frac{2.37\times10^{-5}}{0.779\times3.01\times10^{-5}} = 0.541$

At 250°C: $Sc = \frac{2.54\times10^{-5}}{0.705\times3.62\times10^{-5}} = 0.601$

At 300°C: $Sc = \frac{2.74\times10^{-5}}{0.643\times4.26\times10^{-5}} = 0.663$

At 350°C: $Sc = \frac{2.89\times10^{-5}}{0.592\times5.04\times10^{-5}} = 0.723$

Properties of catalyst

Density = 1.125 g/ml catalyst

Diameter of 100-150 mesh catalyst particle = 0.152 mm

Weight per catalyst particle = $\frac{\pi(0.152\times10^{-1})^3\times1.125}{6} = 2.07\times10^{-6}$ g/particle

External surface area per particle = $\pi(0.152\times10^{-3})^2 = 7.26\times10^{-7}$ m^2/particle

$a_m = \frac{7.26\times10^{-7}}{2.07\times10^{-6}} = 3.51\times10^{-2}$ m^2/gram catalyst

Volumetric flow rate of gaseous feed stream = 100 ml/min

Molar flow rate of gaseous feed stream = $\frac{(1\times10^5)\left(\frac{100\times10^{-6}}{60}\right)}{8.314(273+30)} = 6.62\times10^{-5}$ mol/s

1-propanol molar feed rate = $0.04\times6.62\times10^{-5} = 2.65\times10^{-6}$ mol/s

1-propanol conversion (experimental data): 10% at 200°C

72% at 250°C

98% at 300°C

100% at 350°C

The estimated rate of 1-propanol oxidation reaction is based on the ideal plug-flow reactor which there is no mixing in the direction of flow and complete mixing perpendicular to the direction of flow (i.e., in the radial direction). The rate of reaction will vary with reaction length. Plug flow reactors are normally operated at steady state so that properties at any position are constant with respect to time. The mass balance around plug flow reactor becomes

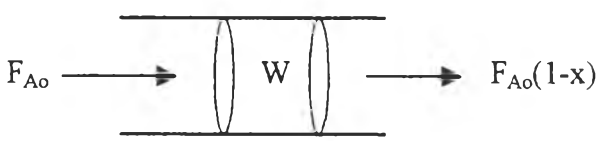

$$\left\{\begin{matrix}\text{rate of i into}\\ \text{volume element}\end{matrix}\right\} - \left\{\begin{matrix}\text{rate of i out of}\\ \text{volume element}\end{matrix}\right\} + \left\{\begin{matrix}\text{rate of production of i within}\\ \text{the volume element}\end{matrix}\right\} = \left\{\begin{matrix}\text{rate of accumulation of i within}\\ \text{the volume element}\end{matrix}\right\}$$

$$F_{Ao} = F_{Ao}(1-x) + (r_w W)$$

$$(r_w W) = F_{Ao} - F_{Ao}(1-x) = F_{Ao}x$$

$$r_w = \frac{F_{Ao}x}{W} = \frac{2.65\times10^{-6}\times0.1}{0.1} = 2.65\times10^{-6} \text{ mol/s-gram catalyst at } 200^{\circ}C$$

$$r_w = \frac{F_{Ao}x}{W} = \frac{2.65\times10^{-6}\times0.72}{0.1} = 1.91\times10^{-5} \text{ mol/s-gram catalyst at } 250^{\circ}C$$

$$r_w = \frac{F_{Ao}x}{W} = \frac{2.65\times10^{-6}\times0.98}{0.1} = 2.59\times10^{-5} \text{ mol/s-gram catalyst at } 300^{\circ}C$$

$$r_w = \frac{F_{Ao}x}{W} = \frac{2.65\times10^{-6}\times1.0}{0.1} = 2.65\times10^{-5} \text{ mol/s-gram catalyst at } 350^{\circ}C$$

At steady state the external transport rate may be written in terms of the diffusion rate from the bulk gas to the surface. The expression is:

$$r_{obs} = k_m a_m (C_b - C_s)$$

$$= \frac{\text{1 – propanol converted (mole)}}{\text{(time)(gram of catalyst)}}$$

where C_b and C_s are the concentrations in the bulk gas and at the surface, respectively.

$$\text{At } 200^\circ\text{C}, \ (C_b - C_s) = \frac{r_{obs}}{k_m a_m} = \frac{2.65 \times 10^{-6}}{0.174 \times 3.51 \times 10^{-2}} = 1.44 \times 10^{-4} \text{ mol/m}^3$$

$$\text{At } 250^\circ\text{C}, \ (C_b - C_s) = \frac{r_{obs}}{k_m a_m} = \frac{1.91 \times 10^{-5}}{0.185 \times 3.51 \times 10^{-2}} = 9.81 \times 10^{-4} \text{ mol/m}^3$$

$$\text{At } 300^\circ\text{C}, \ (C_b - C_s) = \frac{r_{obs}}{k_m a_m} = \frac{2.59 \times 10^{-5}}{0.194 \times 3.51 \times 10^{-2}} = 1.27 \times 10^{-3} \text{ mol/m}^3$$

$$\text{At } 350^\circ\text{C}, \ (C_b - C_s) = \frac{r_{obs}}{k_m a_m} = \frac{2.65 \times 10^{-5}}{0.205 \times 3.51 \times 10^{-2}} = 1.23 \times 10^{-3} \text{ mol/m}^3$$

From C_b (1-propanol) = 1.59 mol/m^3

Consider the difference of the bulk and surface concentration is small. It means that the external mass transport has no effect on the 1-propanol oxidation reaction rate.

B2. Internal diffusional limitation

Next, consider the internal diffusional limitation of the 1-propanol reaction. An effectiveness factor, η, was defined in order to express the rate of reaction for the whole catalyst pellet, r_p, in terms of the temperature and concentrations existing at the outer surface as follows:

$$\eta = \frac{\text{actual rate of whole pellet}}{\text{rate evaluated at outer surface conditions}} = \frac{r_p}{r_s}$$

The equation for the local rate (per unit mass of catalyst) may be expressed functionally as $r = f(C,T)$.

where C represents, symbolically, the concentrations of all the involved components.

Then, $r_p = \eta r_s = \eta f(C_s, T_s)$

Suppose that the 1-propanol oxidation is an irreversible reaction $A \rightarrow B$ and first order reaction, so that for isothermal conditions $r = f(C_A) = k_1 C_A$. Then $r_p = \eta k_1 (C_A)_s$

For a spherical pellet, a mass balance over the spherical-shell volume of thickness Δr. At steady state the rate of diffusion into the element less the rate of diffusion out will equal the rate of disappearance of reactant with in the element. This rate will be $\rho_p k_1 C_A$ per unit volume, where ρ_p is the density of the pellet. Hence, the balance may be written, omitting subscript A on C,

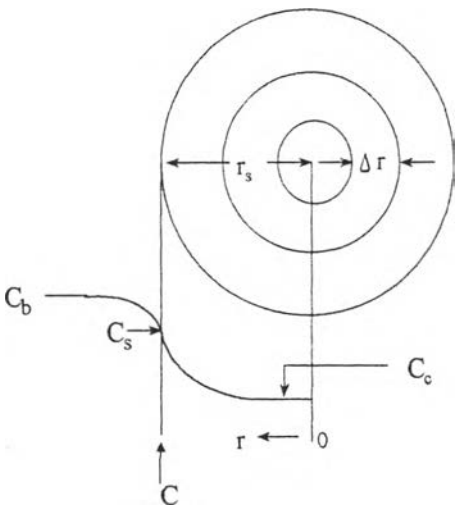

Figure B1 Reactant (A) concentration vs. position for first-order reaction on a spherical catalyst pellet.

$$\left(-4\pi r^2 D_e \frac{dC}{dr}\right)_r - \left(-4\pi r^2 D_e \frac{dC}{dr}\right)_{r+\Delta r} = -4\pi r^2 \Delta r_p k_1 C$$

Take the limit as $\Delta r \rightarrow 0$ and assume that the effective diffusivity is independent of the concentration of reactant, this difference equation becomes

$$\frac{d^2C}{dr^2} + \frac{2dC}{rdr} - \frac{k_1 \rho_p C}{D_e} = 0$$

At the center of the pellet symmetry requires

$$\frac{dC}{dr} = 0 \text{ at } r = 0$$

and at outer surface

$$C = C_s \text{ at } r = r_s$$

Solve linear differential equation by conventional methods to yield

$$\frac{C}{C_s} = \frac{r_s \sinh\left(3\phi_s \frac{r}{r_s}\right)}{r \sinh 3\phi_s}$$

where ϕ_s is Thiele modulus for a spherical pellet defined by $\phi_s = \frac{r_s}{3}\sqrt{\frac{k_1 \rho_p}{D_e}}$

Both D_e and k_1 are necessary to use $r_p = \eta k_1 (C_A)_s$. D_e could be obtained from the reduced pore volume equation in case of no tortuosity factor.

$$D_e = (\varepsilon_s^2 D_{AB})$$

At 200°C , $D_e = (0.5)^2 (3.01\times10^{-5}) = 7.53\times10^{-6}$

At 250°C , $D_e = (0.5)^2 (3.62\times10^{-5}) = 9.04\times10^{-6}$

At 300°C , $D_e = (0.5)^2 (4.26\times10^{-5}) = 1.06\times10^{-5}$

Substitute radius of catalyst pellet , $r_s = 0.076\times10^{-3}$ m with ϕ_s equation

$$\phi_s = \frac{0.076\times10^{-3}\,m}{3}\sqrt{\frac{k(m^3/s - kg\ cat.)\times 1125(kg/m^3)}{7.53\times10^{-6}(m^2/s)}},\ \text{at } 200^\circ C$$

$\phi_s = 0.310\sqrt{k}$ (dimensionless) at 200°C

$\phi_s = 0.283\sqrt{k}$ (dimensionless) at 250°C

$\phi_s = 0.261\sqrt{k}$ (dimensionless) at 300°C

Find k (at 200°C) from the mass balance equation around plug-flow reactor.

$$r_w = \frac{F_{Ao}dx}{dW}$$

where $r_w = kC_A$

Thus, $$kC_A = \frac{F_{Ao}dx}{dW}$$

$$kC_{Ao}(1-x) = \frac{F_{Ao}dx}{dW}$$

$$W = \frac{F_{Ao}}{kC_{Ao}} \int_0^{0.1} \frac{1}{1-x} dx$$

$$W = \frac{F_{Ao}}{kC_{Ao}} \left[-\ln(1-x) \right]_0^{0.1} = \frac{F_{Ao}}{kC_{Ao}} (-\ln(0.9))$$

$$k = \frac{F_{Ao}}{WC_{Ao}} (-\ln(0.9))$$

$$k = \frac{2.65 \times 10^{-6} \ (\text{mol/s})}{0.1 \times 10^{-3} (\text{kg}) \times 1.59 (\text{mol/m}^3)} (-\ln(0.9))$$

$$= 1.76 \times 10^{-3} \ \text{m}^3/\text{s-kg catalyst}$$

Calculate ϕ_s: $\phi_s = 0.310\sqrt{1.76 \times 10^{-3}} = 0.013$ at 200°C

$\phi_s = 0.286\sqrt{2.12 \times 10^{-2}} = 0.042$ at 250°C

$\phi_s = 0.261\sqrt{6.52 \times 10^{-2}} = 0.067$ at 300°C

For such small values of ϕ_s it was concluded that the internal mass transport has no effect on the rate of 1-propanol oxidation reaction.

APPENDIX C

GAS CHROMATOGRAPH

C1 Operating condition

Flame ionization detector gas chromatographs, model 14A and 14B, were used to analyze the concentrations of oxygenated compounds and light hydrocarbons, respectively, 1-propanol, propanal and formaldehyde were analyzed by GC model 14A while methane, ethene, propane and propene were analyzed by GC model 14B.

Gas chromatograph with the thermal conductivity detector, model 8A was used to analyze the concentrations of CO_2 and CO by using Porapak QS and Molecular Sieve 5A column, respectively.

The operating conditions for gas chromatograph are described below:

GC model	**Shimadzu GC-14B**	**Shimadzu GC-14A**	**Shimadzu GC-8A**
Detector	FID	FID	TCD
Column	VZ-10	Capillary	Porapak QS and Molecular sieve 5A
Nitrogen flow rate	60 ml/min	25 ml/min	-
Helium flow rate	-	-	25 ml/min
Column temperature			
- initial	55°C	35°C	80°C
- final	65°C	140°C	80°C
Injection temperature	100°C	150°C	130°C
Detector temperature	150°C	150°C	130°C

C2 Calibration curve

The calibration curves of methane, ethene, propane, propene, 1-propanol, formaldehyde, propanal, CO and CO_2 are illustrated in the following figures.

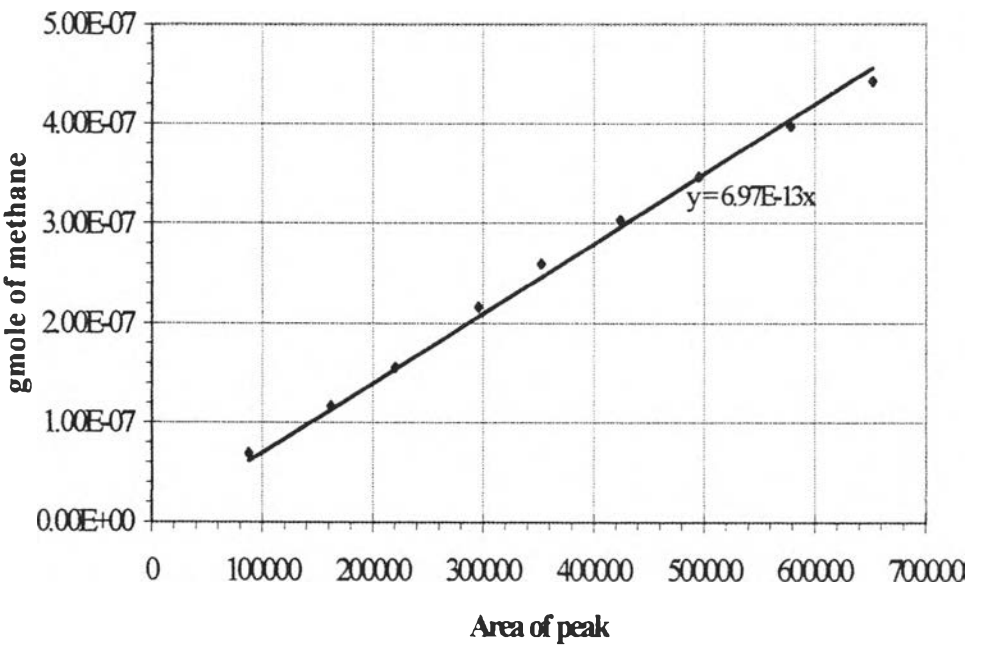

Figure C1 The calibration curve of methane

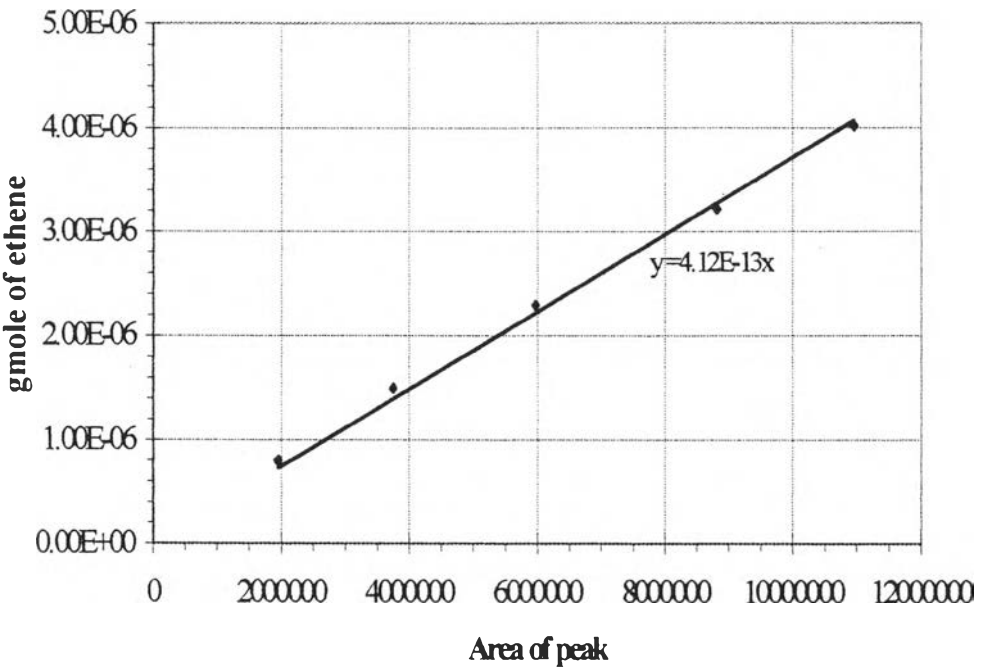

Figure C2 The calibration curve of ethene

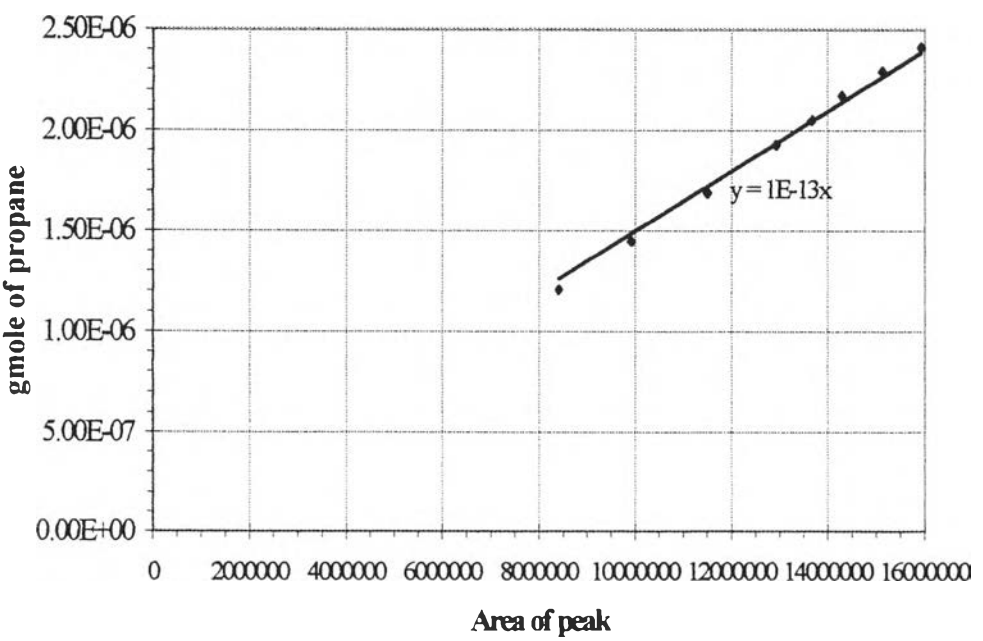

Figure C3 The calibration curve of propane

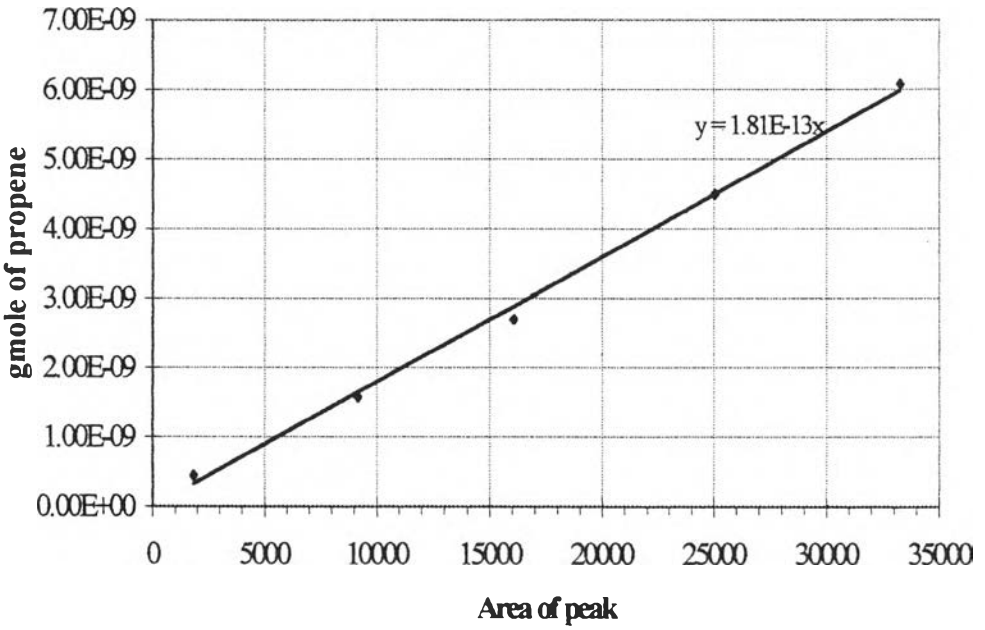

Figure C4 The calibration curve of propene

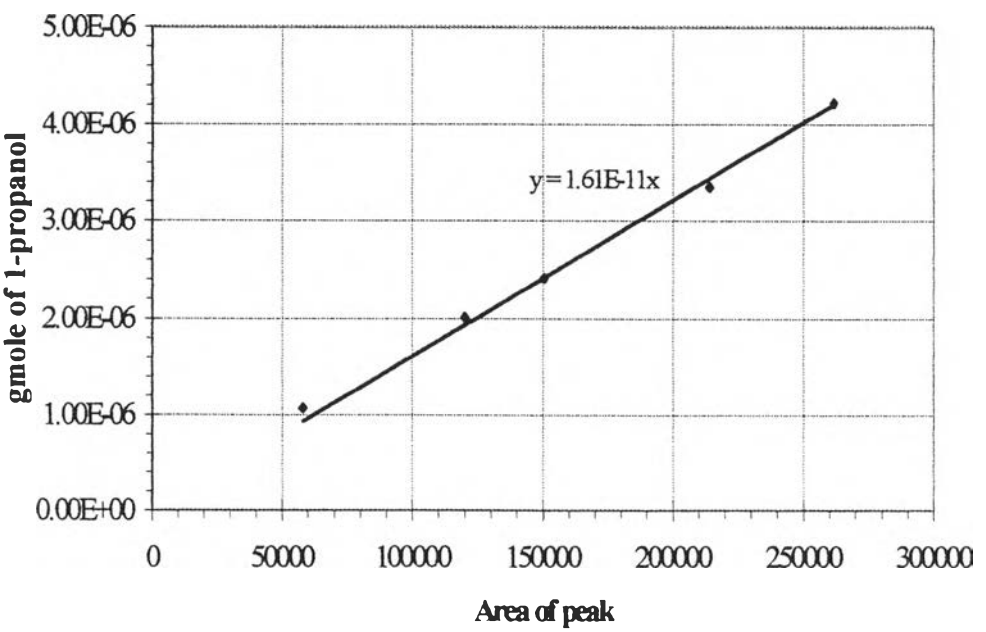

Figure C5 The calibration curve of 1-propanol

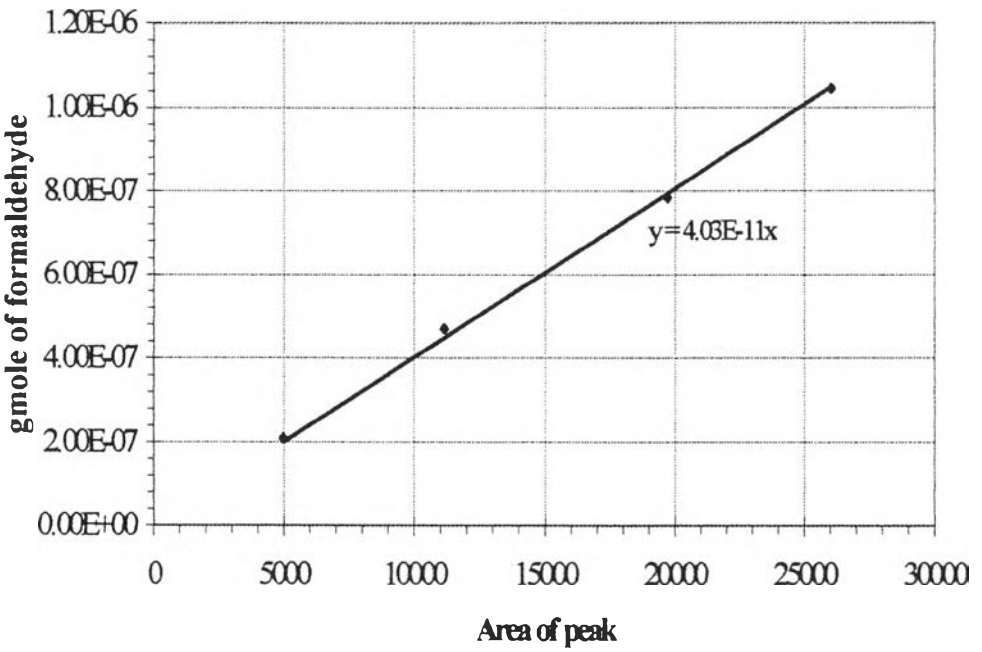

Figure C6 The calibration curve of formaldehyde

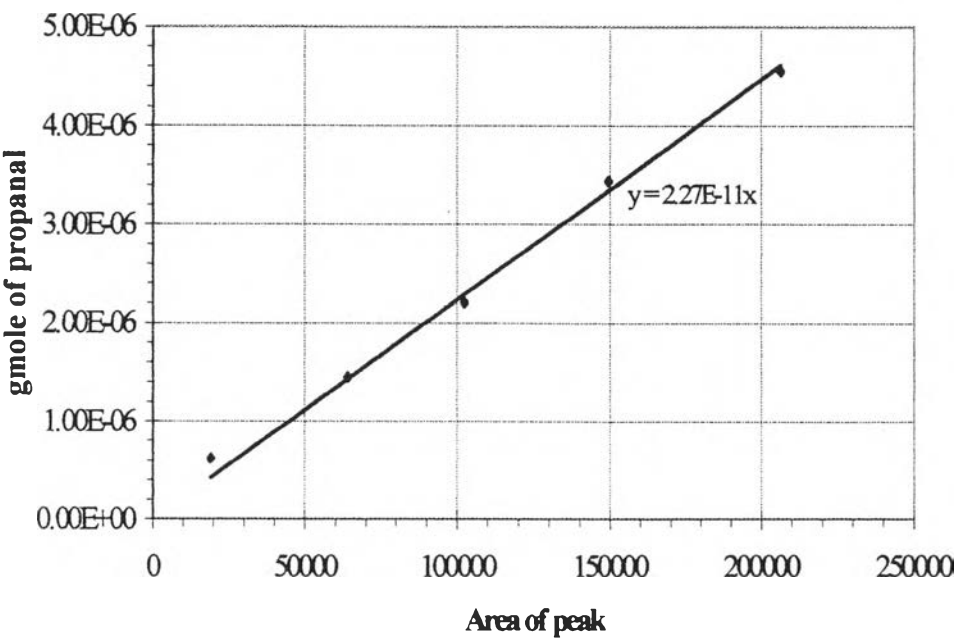

Figure C7 The calibration curve of propanal

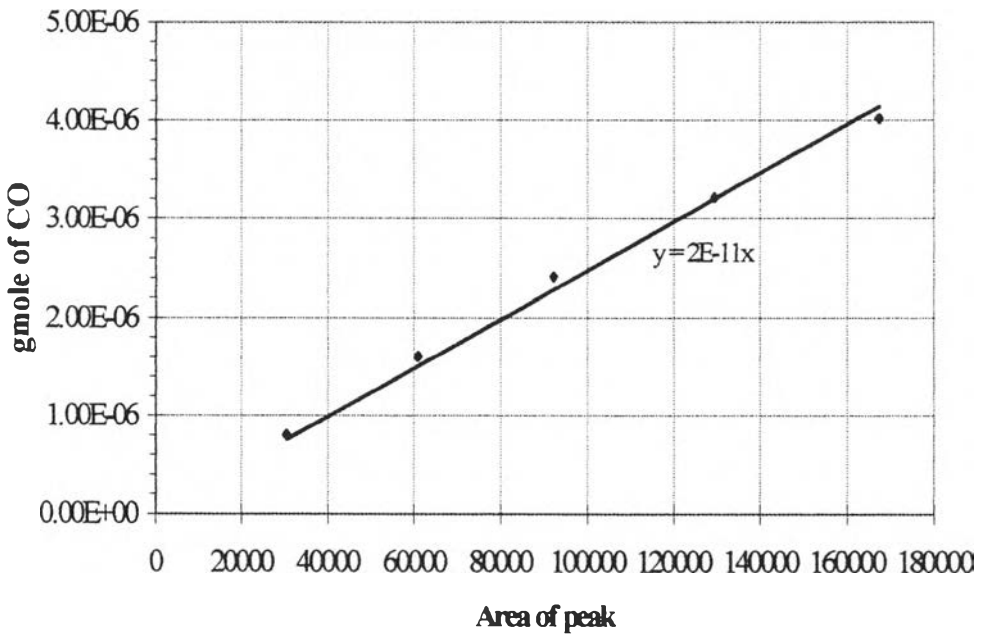

Figure C8 The calibration curve of CO

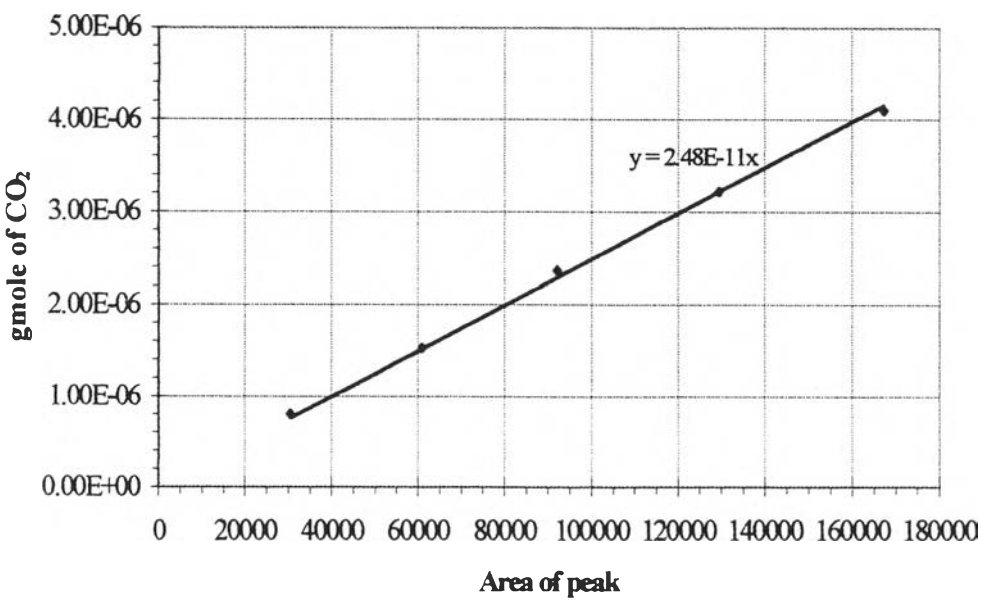

Figure C9 The calibration curve of CO_2

C3 Samples of chromatogram

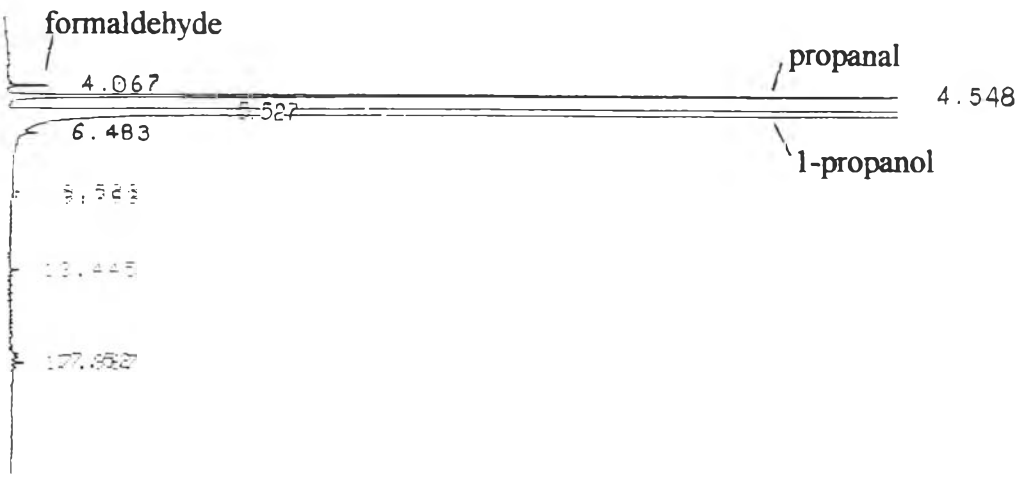

Figure C10 Sample of chromatogram from GC-14A

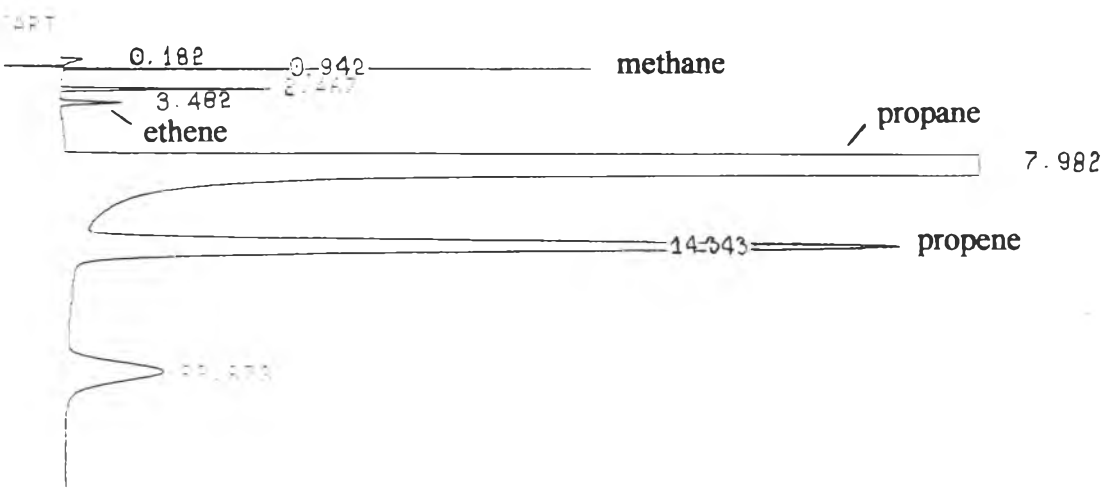

Figure C11 Sample of chromatogram from GC-14B

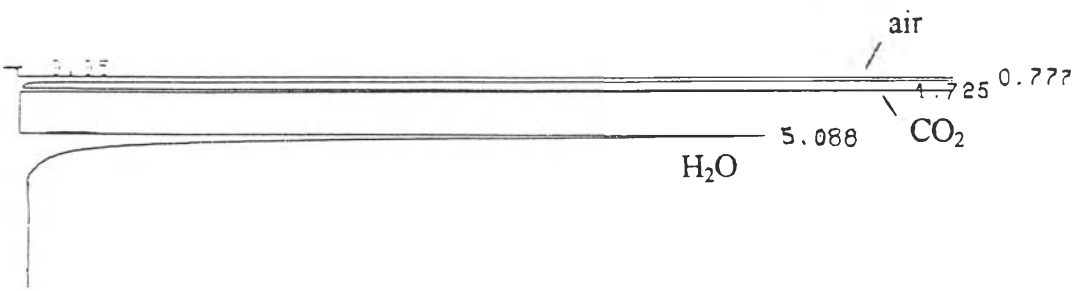

Figure C12 Sample of chromatogram from GC-8A (Porapak QS column)

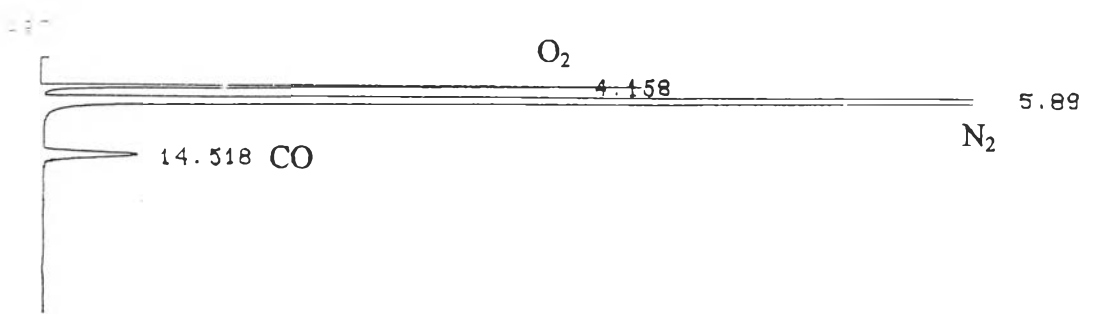

Figure C13 Sample of chromatogram from GC-8A (Molecular Sieve 5A column)

APPENDIX D

DATA OF EXPERIMENT

Table D1 Data of figure 5.18

Temperature (°C)	$\%C_3H_8$ conversion	$\%CH_4$ selectivity	$\%C_2H_4$ selectivity	$\%C_3H_6$ selectivity	$\%CO_2$ selectivity
300	0.2	0	0	11.4	88.6
350	0.7	0	0	8.9	91.1
400	1.2	0	0	10.5	89.5
425	2.2	0	0	10.0	90.0
450	3.5	0	0.1	9.4	90.5
475	6.3	0	0.2	8.0	91.9
500	10.2	0	0.4	7.4	92.5

Table D2 Data of figure 5.19

Temperature (°C)	$\%C_3H_8$ conversion	$\%CH_4$ selectivity	$\%C_2H_4$ selectivity	$\%C_3H_6$ selectivity	$\%CO_2$ selectivity
350	0.1	0.0	0.0	22.1	77.5
400	0.8	0.0	1.2	21.6	78.4
425	1.4	0.9	1.4	22.6	76.6
450	3.0	0.7	1.6	23.9	78.2
475	4.5	0.5	1.4	23.4	78.2
500	5.3	0.5	1.4	22.8	76.1

Table D3 Data of figure 5.20

Temperature (°C)	$\%C_3H_8$ conversion	$\%CH_4$ selectivity	$\%C_2H_4$ selectivity	$\%C_3H_6$ selectivity	$\%CO_2$ selectivity
350	0.4	0.0	0.0	17.6	81.0
400	0.8	0.5	1.5	19.0	81.2
425	1.4	0.9	1.8	18.4	79.0
450	2.6	0.7	2.0	19.0	79.2
475	3.4	0.5	1.7	18.4	79.4
500	5.4	0.5	1.6	19.6	79.1

Table D4 Data of figure 5.21

Temperature (°C)	$\%C_3H_8$ conversion	$\%CH_4$ selectivity	$\%C_2H_4$ selectivity	$\%C_3H_6$ selectivity	$\%CO_2$ selectivity
350	0.2	2.3	0.0	12.0	85.7
400	0.9	0.3	0.0	12.9	86.8
425	1.6	0.0	0.5	13.2	86.0
450	2.8	0.0	0.8	12.8	86.1
475	3.5	0.1	0.9	13.2	85.7
500	5.0	0.0	1.2	12.7	86.1

Table D5 Data of figure 5.22

Temperature (°C)	$\%C_3H_8$ conversion	$\%CH_4$ selectivity	$\%C_2H_4$ selectivity	$\%C_3H_6$ selectivity	$\%CO_2$ selectivity
350	0.2	0.0	0.0	30.9	69.1
400	0.8	1.4	0.0	27.9	70.7
425	1.7	0.6	0.6	26.5	72.1
450	2.8	0.5	0.6	28.5	69.0
475	3.9	0.8	0.8	27.0	72.0
500	5.7	1.1	0.1	27.5	71.9

Table D6 Data of figure 5.23

Temperature (°C)	$\%C_3H_8$ conversion	$\%CH_4$ selectivity	$\%C_2H_4$ selectivity	$\%C_3H_6$ selectivity	$\%CO_2$ selectivity
300	0	0	0	0	0
400	0.2	1.0	0.0	22.1	76.3
425	0.4	0.7	0.0	24.3	74.9
450	2.4	0.5	0.0	26.3	73.2
475	3.3	0.4	0.0	28.6	71.1
500	3.9	0.8	0.6	27.9	71.3

Table D7 Data of figure 5.24

Temperature (°C)	$\%C_3H_8$ conversion	$\%CH_4$ selectivity	$\%C_2H_4$ selectivity	$\%C_3H_6$ selectivity	$\%CO_2$ selectivity
350	0.5	0	0.0	23.1	76.9
400	1.8	0	0.0	25.2	74.8
425	2.6	0	0.0	30.2	69.8
450	3.5	0	0.0	31.4	68.6
475	4.6	0.2	0.3	35.5	64.2
500	6.5	0.3	0.6	40.8	58.5

Table D8 Data of figure 5.28

Temperature (°C)	$\%C_3H_6$ conversion	$\%C_3H_6O$ selectivity	$\%CO_2$ selectivity
300	0	0	0
350	0	0	0
400	2.3	73.1	22
450	4.2	72.6	23.6
500	5.8	71	26.1

Table D9 Data of figure 5.29

Temperature (°C)	$\%C_3H_7OH$ conversion	$\%C_2H_4$ selectivity	$\%C_3H_6$ selectivity	$\%CH_2O$ selectivity	$\%C_3H_6O$ selectivity	$\%CO_2$ selectivity
200	63.0	0	0.3	1.8	47.0	41.8
250	99.7	0	11.4	8.1	5.5	54.1
300	99.9	0	14.0	4.4	1.7	60.5
350	100	0	20.9	2.5	1.2	63.3
400	100	0.3	22.8	1.6	0.8	70.3
450	100	0.8	26.6	2.0	0.7	67.8
500	100	2.6	28.4	1.3	0.5	63.6

Table D10 Data of figure 5.30

Temperature (°C)	%C_3H_7OH conversion	%C_2H_4 selectivity	%C_3H_6 selectivity	%CH_2O selectivity	%C_3H_6O selectivity	%CO_2 selectivity
200	5.5	0	0	1.5	96.9	1.5
250	35.2	0	0.7	5.0	87.8	2.7
300	95.8	0	4.2	11.2	16.1	56.7
350	99.7	0	9.8	4.9	3.6	66.9
400	99.9	0	20.9	1.4	2.5	67.9
450	100	2.3	31.1	0	1.8	60.3
500	100	8.7	33.0	0	1.4	56.1

Table D11 Data of figure 5.31

Temperature (°C)	%C_3H_7OH conversion	%C_2H_4 selectivity	%C_3H_6 selectivity	%CH_2O selectivity	%C_3H_6O selectivity	%CO_2 selectivity
200	5.5	0	0	1.7	94.6	3.6
250	48.7	0	0.6	6.6	82.7	5.4
300	95.4	0	2.2	11.8	18.3	62.7
350	99.7	0	6.2	4.7	0.9	83.8
400	99.9	0.1	16.8	1.2	1.5	80.0
450	100	0.5	23.8	0.6	1.1	71.8
500	100	5.3	30.1	0	0.9	60.6

Table D12 Data of figure 5.32

Temperature (°C)	%C_3H_7OH conversion	%C_2H_4 selectivity	%C_3H_6 selectivity	%CH_2O selectivity	%C_3H_6O selectivity	%CO_2 selectivity
200	4.4	0	0	1.9	96.4	1.5
250	30.0	0	1.4	2.3	86.6	3.8
300	99.5	0	9.6	8.2	13.7	63.2
350	100	0.4	14.2	2.3	6.1	71.5
400	100	0.6	20.2	1.3	1.9	68.0
450	100	0.9	25.8	0.9	1.8	66.5
500	100	3.5	29.6	0	1.3	59.0

Table D13 Data of figure 5.33

Temperature (°C)	%C_3H_7OH conversion	%C_2H_4 selectivity	%C_3H_6 selectivity	%CH_2O selectivity	%C_3H_6O selectivity	%CO_2 selectivity
200	1.5	0	0	1.6	98.5	0
250	13.2	0	0.7	1.5	81.0	15.9
300	99.7	0	17.1	6.8	8.0	66.8
350	99.9	0	22.6	2.6	4.8	64.3
400	100	1.3	23.7	1.5	4.0	63.5
450	100	2.7	28.8	0.9	2.7	61.3
500	100	4.8	36.5	0	1.5	56.8

Table D14 Data of figure 5.34

Temperature (°C)	%C_3H_7OH conversion	%C_2H_4 selectivity	%C_3H_6 selectivity	%CH_2O selectivity	%C_3H_6O selectivity	%CO_2 selectivity
200	6.0	0	0	1.4	96.9	1.1
250	39.0	0	1.2	3.8	92.8	1.9
300	98.8	0	10.9	4.8	14.0	63.7
350	99.6	0	11.4	9.3	5.4	69.0
400	99.8	0.4	15.9	1.5	4.1	77.4
450	100	1.0	19.3	0	2.4	75.7
500	100	2.8	27.8	0	0.2	70.1

Table D15 Data of figure 5.35

Temperature (°C)	%C_3H_7OH conversion	%C_2H_4 selectivity	%C_3H_6 selectivity	%CH_2O selectivity	%C_3H_6O selectivity	%CO_2 selectivity
200	10.0	0	0.1	2.1	96.5	0.7
250	72.0	0	2.8	14.9	68.0	8.4
300	97.8	0	16.8	8.7	17.9	47.8
350	100	0	24.2	4.0	11.1	52.0
400	100	2.2	31.0	2.0	8.3	48.7
450	100	3.0	38.6	0	6.9	46.3
500	100	9.4	41.6	0	5.8	39.8

Table D16 Data of figure 5.36

Temperature (°C)	CO conversion
250	0.0
300	0.9
350	2.3
400	3.9
450	5.1
500	8.8

APPENDIX E

PUBLISHED PAPER

This published emerged during this study was presented at Academic Conference, 8th, Mahidol University, 17-18 December 1998.

คุณสมบัติในการออกซิเดชันของตัวเร่งปฏิกิริยาวาเนเดียมแมกนีเซียมออกไซด์บนตัวรองรับไทเทเนียมออกไซด์

นางสาวระพีพรรณ เล็กเลิศสุนทร, ผศ.ดร. ธราธร มงคลศรี
ภาควิชาวิศวกรรมเคมี คณะวิศวกรรมศาสตร์
จุฬาลงกรณ์มหาวิทยาลัย กรุงเทพฯ 10330

บทคัดย่อ

การทดลองได้ทำการศึกษาผลของการเติมแมกนีเซียมลงในตัวเร่งปฏิกิริยาวาเนเดียมออกไซด์-ไทเทเนียมออกไซด์ที่มีต่อคุณสมบัติการออกซิเดชันของวาเนเดียมออกไซด์โดยใช้ปฏิกิริยาออกซิเดชันของโพรเพน ผลิตภัณฑ์หลักที่พบคือ โพรพีน และคาร์บอนไดออกไซด์ จากการศึกษาพบว่าลำดับการเติมแมกนีเซียมและปริมาณแมกนีเซียมที่เติมลงไปมีผลต่อคุณสมบัติของตัวเร่งปฏิกิริยาดังกล่าว นอกจากนี้ยังพบว่าค่าเลือกเกิดของทั้งโพรพีนและคาร์บอนไดออกไซด์มีค่าค่อนข้างคงที่ ไม่เปลี่ยนแปลงตามอุณหภูมิ แสดงว่าเส้นทางของการเกิดโพรพีนเป็นคนละเส้นทางกับของการเกิดคาร์บอนไดออกไซด์

Oxidation properties of V-Mg-O on TiO_2 support

Rapeepun Leklertsunthorn, Tharathorn Monkhonsi*
Petrochemical Engineering Laboratory, Department of Chemical Engineering,
Chulalongkorn University, Bangkok 10330 Thailand.
*To whom correspondance should be addressed

Abstract

Vanadium (V) oxide has been known to show strong interaction between titanium oxide and several supports. In this paper, the Mg-doped V_2O_5/TiO_2 catalysts were prepared to study the oxidation property of vanadium oxide. The propane oxidation reaction was used as a test reaction. Propene and CO_2 were found to be the main products. It was found that the sequence of Mg introduction to V_2O_5/TiO_2 system and Mg content have some effects on catalytic performance of catalysts. Moreover, it was observed that the selectivity to propene and CO_2 of these catalysts were independent of temperature. Consequently, the pathway of propene and CO_2 formation may be different.

Keywords: Propane oxidation, Mg-doped V_2O_5/TiO_2 catalysts

1. Introduction

Supported vanadium oxides are widely used as catalysts for many hydrocarbon oxidation reactions. The activity and selectivity of these catalysts depend on the supports. The acidity-basicity of supported used can control structure of vanadium oxide species on the support surface, leading to different catalytic properties. On acidic support such as TiO_2 anatase vanadium oxide prefers to insert oxygen atom(s) into hydrocarbon molecules. This catalytic system has been used in several partial oxidation of o-xylene to phthalic anhydride and butane or butene to maleic anhydride. In contrast, V_2O_5 supported on basic support, MgO, presents different catalytic properties. It is known that vanadium oxide reacts with MgO to form new V-Mg-O compound, not form vanadium oxides on Mg surface [Chaar et al. (1987, Sam et al (1990), Okuhara et al. (1993)]. On this support, vanadium oxide tends to remove hydrogen atoms in form of water from reactant without insertion any oxygen atoms into reactant. This V-Mg-O system was found to be active and selective for oxidative dehydrogenation of butane [Chaar et al. (1987)] and propane [Chaar et al. (1988)]. Furthermore, Bhattacharyya et al. (1992) have investigated the effect of TiO_2 added to V-Mg-O catalyst for the selective oxidation of n-butane to butadiene. They proposed that the catalyst 24V-Mg-O incorporating TiO_2 provided not only higher activity but also better selectivity.

In this research, we tried to deposit Mg on V_2O_5/TiO_2 catalyst to investigate the oxidation property of vanadium oxide. The effect of sequence of Mg introduction and the Mg content on V_2O_5/TiO_2 were obtained.

2. Experimental

2.1 Catalyst preparation

The V_2O_5/TiO_2 catalysts were prepared by the conventional wet impregnation using pure TiO_2 (Farmitalia Carlo Erba) as support. The TiO_2 powder was added to an aqueous solution containing an appropriate amount of ammonium metavanadate, NH_4VO_3 (Farmitalia Carlo Erba).

Fives series of Mg-V_2O_5/TiO_2 catalysts were prepared. The first three type samples contain 5 wt% vanadium oxide (calculated as V_2O_5) and M/V atomic ratio equal to 1/1. The difference betweem them was sequence of Mg introduction. The first type of preparation, TiO_2 (anatase) was added to an aqueous solution of NH_4VO_3. With stirring, the suspension was evaporated to dryness, followed by calcination in air at 550°C for 6 hr. Mg was then introduced onto the sample by impregnation from a $Mg(NO_3)_2$ solution, evaporating and calcination in air at 550°C for 6 hr. This sample was denoted as 5VMgTi[1/1]. The second type of sample, denoted as Mg5VTi[1/1], was prepared by the same method of 5VMg/Ti[1/1], but magnesium was first introduced to pure TiO_2 and then vanadia was deposited on Mg-doped TiO_2 support. For sample denoted by the symbol co-5VMg/Ti[1/1], the titania was added to an aqueous solution containing NH_4VO_3 and $Mg(NO_3)_2$. The suspension was dried and then the resulting solid was calcined in the same above condition.

The last two type samples, 5VMgTi[1/2] and 5VMgTi[3/2], were prepared. The Mg/V atomic ratio were 1/2 and 3/2, respectively. Vanadia was first introduced on to pure TiO_2 and then Mg was deposited on calcined V_2O_5/TiO_2 sample. The steps of preparation were the same as that of 5VMgTi[1/1] catalyst.

2.2 Catalyst Characterization

The crystal structure of samples was characterized by XRD using SIEMENS D500 diffractometer with CuKα radiation.

All samples were characterized by FT-IR using Nicolet model Impact 400. Each sample was prepared by mixing and appropriate amount of the catalyst with KBr to form a thin wafer for IR characterization.

The propane oxidation was used as test reaction. The reaction was carried out in a quartz tubular fixed bed micro reactor system under atmospheric pressure. Propane and air were used as reactant. Propane and oxygen concentration were controlled at 4 and 20 vol% respectively. Effluent gas was analyzed using gas chromatograph Shimadzu model 14B equipped with a flame ionization and a VZ-10 column and Shimadzu model 8A equipped with a thermal conductivity detector and Porapak QS column.

3. Results and Discussion

3.1 X-ray Diffraction

X-ray diffraction patterns of all catalysts are illustrated in Fig. 1. Only diffraction line of TiO_2 can be observed. It can be seen that V_2O_5 peak cannot be detected. That means that the amount of vanadium oxides on TiO_2 surface may be not enough to be determined by XRD or the vanadium oxides did not form a V_2O_5 crystal structure on the TiO_2 support. In reality it is known that, at low V loading, vanadium oxide possibly form only thin layer distributed on the surface of titania. [Nieto et al. (1990), Bond et al. (1991)]. In addition, Magnesium oxide peaks were not found on all catalysts. It may be due to the magnesium content loaded is much less

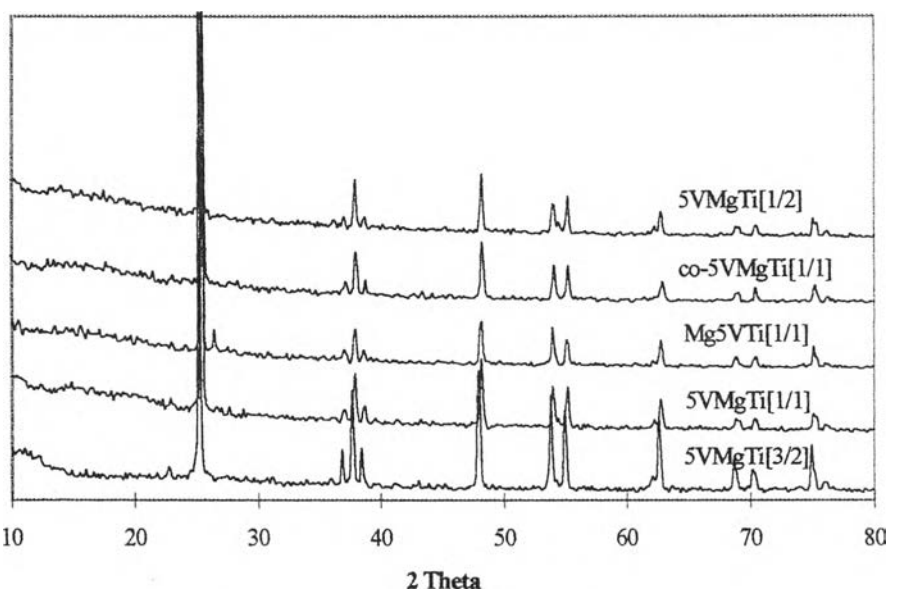

Figure 1 XRD patterns of all catalysts

3.2 Infrared Spectroscopy.

Figure 2 shows IR spectra of all catalysts. All spectrum are similar and show strong absorption IR bands at 580 and 680 cm-1 that belong to TiO_2. The weak band assigned to MgO appears at 1123 cm-1, but it is not clear due to low Mg loading.

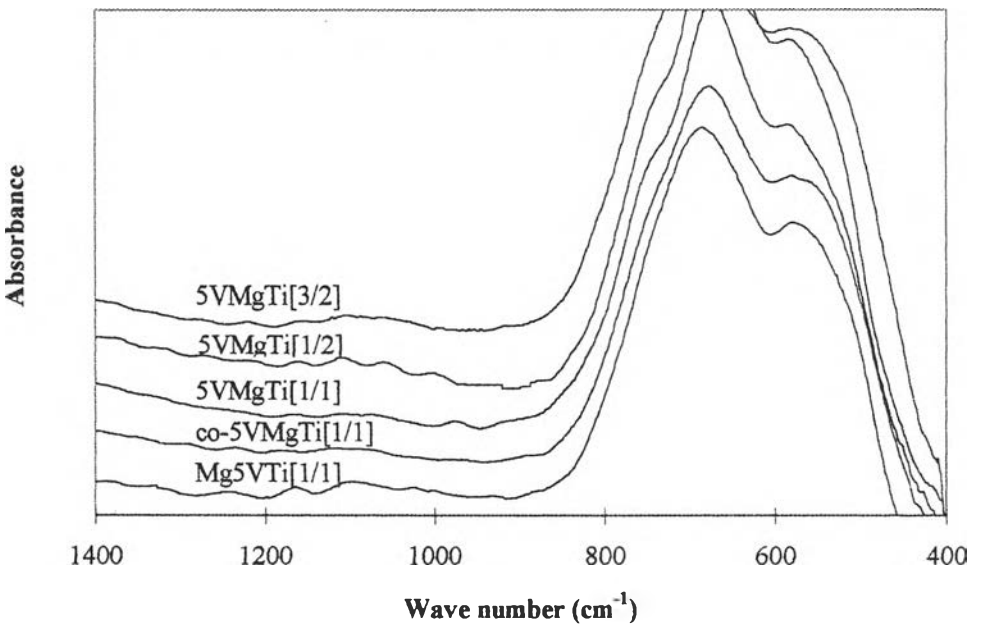

Figure 2 IR spectra of all catalysts

3.3 Catalytic Test

In propane oxidation reaction, propene and carbon dioxide are the major products. The amount of C1, C2 hydrocarbons are below 3% of total products. Although the conversion increases with rise in temperature, it is quite low. Therefore, it is neglected to shown conversion here.

The selectivity as a function of temperature is demonstrated in Figs. 3 to 7. It can be seen that, for catalysts with Mg/V atomic ratio equals to 1/1, 5VMgTi[1/1] (Fig. 5) presents the highest selectivity to propene, while the selectivity of co-5VMgTi [1/1] (Fig. 3) is lower, and that of Mg5VTi[1/1] (Fig. 4) is the lowest. From these results, it can be suggested that the sequence of Mg loading on V_2O_5/TiO_2 catalysts has an influence on catalytic performance of these catalysts.

Figures 6 and 7 illustrate the effect of Mg contents on the performance of 5VMgTi catalysts. It was found that propene and CO_2 selectivity of 5VMgTi[1/2] (Fig.6) and 5VMgTi[1/1] (Fig. 7) are similar, while that of 5VMgTi[3/2] (Fig. 5) is slightly increased.

On V-Mg-O system, the propene selectivity rapidly decreases with increase in temperature [Thammanonkul (1996), Kanokrattana (1998)]. In contrast, for Mg-doped V_2O_5/TiO_2 catalysts, they have the benefit of constant selectivities, being independent with temperature. If propene is further oxidised to form CO_2, the selectivity to propene should decrease while that of CO_2 should increase with the increase in temperature. Therefore it may be suggested that the pathway of propene formation is not the same as that of CO_2 formation.

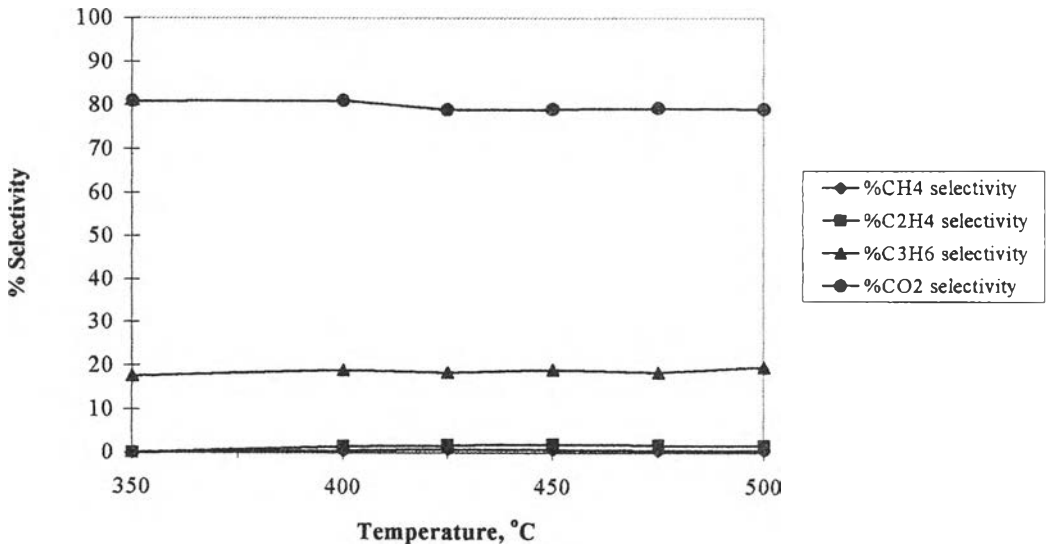

Figure 3 Catalytic property of co-5VMgTi[1/1]

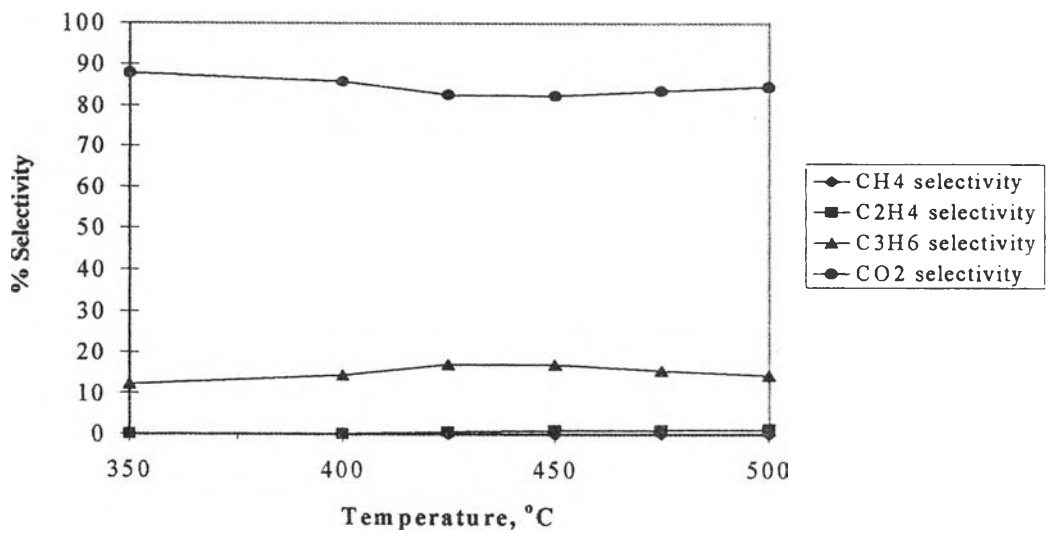

Figure 4 Catalytic property of Mg5VTi[1/1]

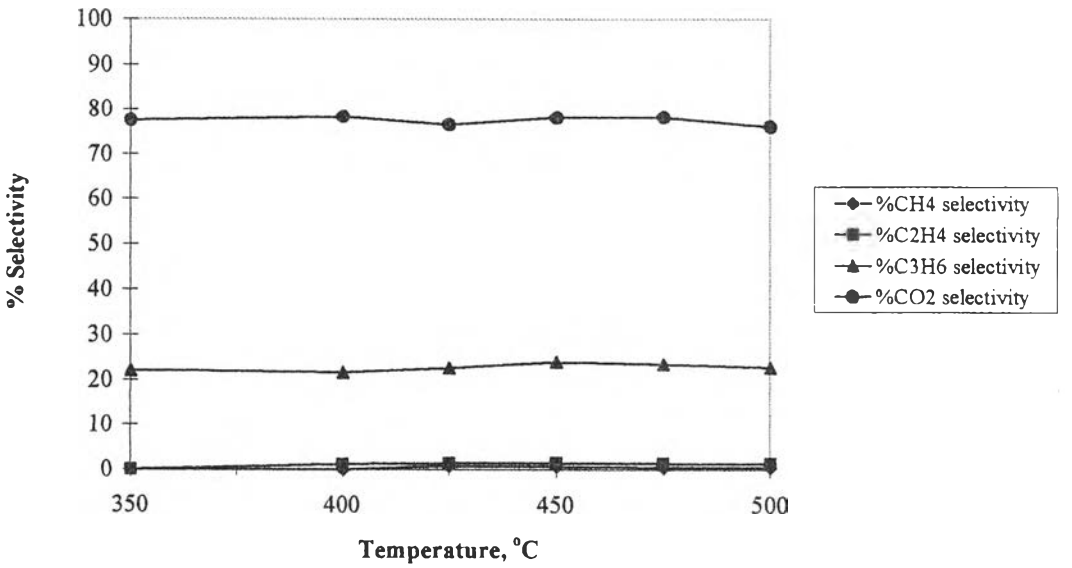

Figure 5 Catalytic property of 5VMgTi[1/1]

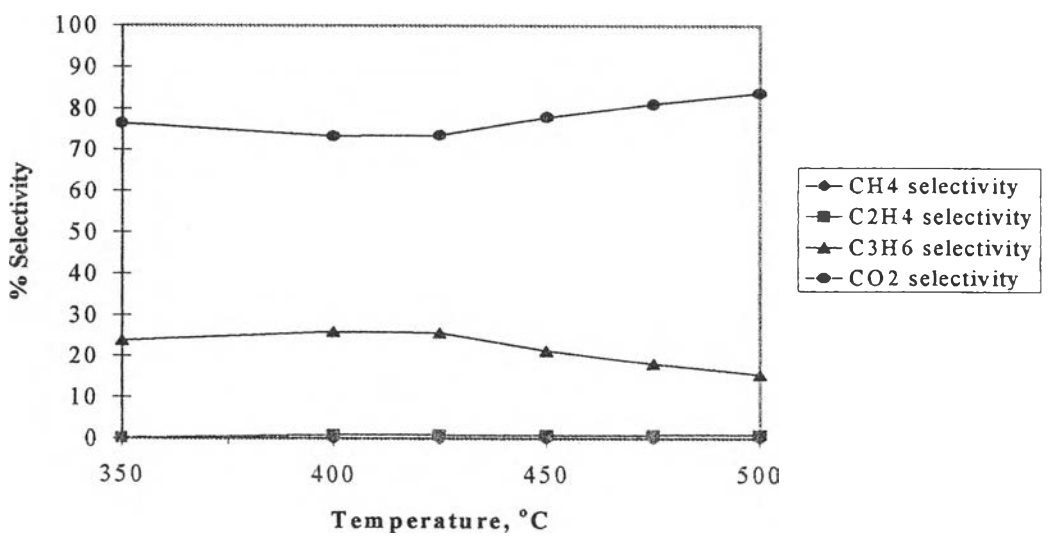

Figure 6 Catalytic property of 5VMgTi[1/2]

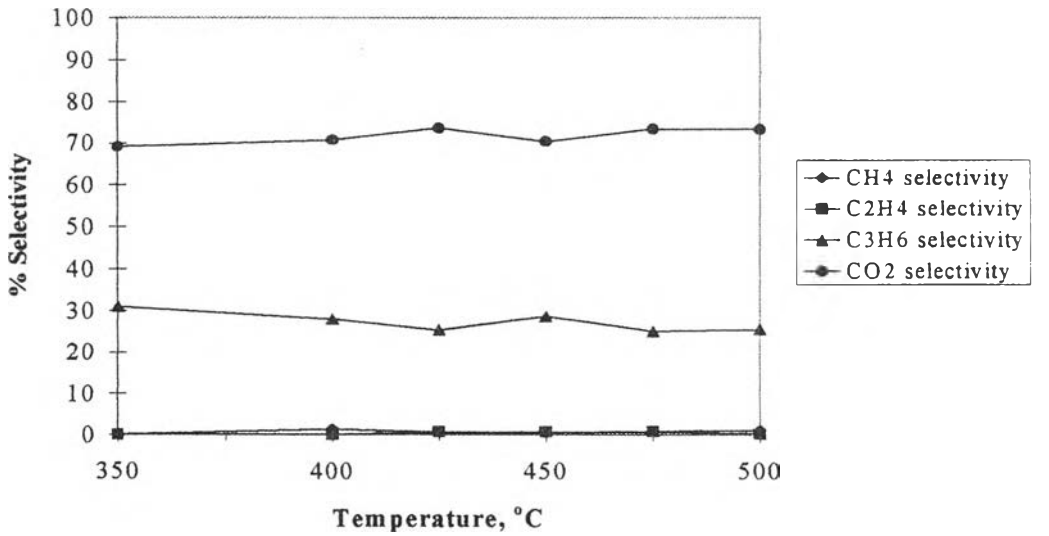

Figure 7 Catalytic property of 5VMgTi[3/2]

4. Conclusions

The influence of Mg deposition to V_2O_5/TiO_2 system on catalytic property of catalysts in propane oxidation reaction:

1. The sequence of introduction of the magnesium additive to V_2O_5/TiO_2 has some effect on propene selectivity. Catalyst with the highest selectivity to propene is 5VMgTi catalyst as compare with the Mg5VTi and co-5VMgTi catalysts.

2. The propene and CO_2 selectivity of all catalysts were independent of temperature. Thus the pathway of propene and CO_2 formation may be different.

Acknowledgement

The authors would like to thank Thailand Research Fund (TRF) for financial support and Prof. Piyasan Praserthdam for his helpful suggestion.

References

Bhattacharyya, D., Shyamal K. Bej and Musti S. Rao, "Oxidative dehydrogenation of n-butane to butadiene. Effect of different promoters on the performace of vanadium-magnesium oxide catalysts", *Appl. Catal.*, **87**, 29(1992)

Bond, G.C., "Vanadium oxide monolayer catalysts Preparation, characterization and catalytic activity", *Appl. Catal.*, **71**, 1(1991)

Chaar, M.A., Patel, D., and Kung, H.H., "Selective Oxidative Dehydrogenation of Butane over V-Mg-O Catalysts", *J.Catal.*, **105**, 483(1987)

Chaar, M.A., Patel, D., and Kung, H.H., "Selective Oxidative Dehydrogenation of Propane over V-Mg-O Catalysts", *J.Catal.*, **109**, 463(1988)

Hongsuda Thammononkul, "Oxidative dehydrogenation of propane over V-Mg-O catalysts", *Master of Engineering thesis*, Chulalongkorn University (1996)

López Nieto, J.M., Kremenic,G., Fierro, J.L.G., "Selective Oxidation of Propene over Supported Vanadium Oxide Catalysts", *Appl. Catal.*, **61**, 235(1990)

Orawan Kanokrattana,"Effects of alkali metals on V-Mg-O catalyst in the oxidative dehydrogenation of propane", *Master of Engineering thesis*, Chulalongkorn University, (1997)

Okuhara, T., Inumaru, K., Misono,M., Matsubayashi, N., Shimada, H., and Nishijima, A., "Structures and dehydrogenation activities of vanadium oxide overlayers on supports", *Catal. Letters*, **20**, 73(1993)

Sam, D.S.H., Soenen, V., and Volta, J.C., "Oxidative Dehydrogenation of Propane over V-Mg-O Catalysts", *J. Catal.*, **123**, 417(1990)

VITA

Miss Rapeepun Leklertsunthorn was born in Lampang on December 29, 1976. She graduated high school from Bunyawat Wittayalai School, Lampang in 1992 and received her Bachelor degree of Chemical Engineering from the Faculty of Engineering, Chulalongkorn University in 1996.